

# Neutron Characterization and Calphad in support of the Metal Hydride Center of Excellence

Terrence J. Udovic  
Ursula R. Kattner  
Hui Wu  
Mohammed Yousufuddin

June 9<sup>th</sup> 2008



NIST

**National Institute of Standards and Technology**  
Technology Administration, U.S. Department of Commerce

STP-7

## Timeline

- Project start FY05
- Project end FY09
- 70% complete

## Budget

<u>FY</u>	<u>HSCoE</u>	<u>MHCoE</u>
• FY05	\$130K	\$125K
• FY06	\$208K	\$156K
• FY07	\$216K	\$276K
• FY08	\$225K	\$287K

NIST continues to provide access to neutron facilities and FTEs for the HSCoE and MHCoE

## Barriers addressed

- A. System Weight and Volume
- P. Lack of Understanding of Hydrogen Physisorption and Chemisorption

## Partners

- Sandia, JPL, HRL, Caltech, Hawaii, Stanford, Nevada-Reno, Maryland, Michigan, Washington U.  
– **Neutron-based Characterization**
- Carnegie Mellon, Pittsburgh, HRL, Illinois, Missouri-St. Louis  
– **Calphad Calculations**
- Sandia  
– **Project Lead**

**Overall:** Support the development of hydrogen-storage materials by providing timely, comprehensive characterization of Center-developed materials and storage systems using state-of-the-art neutron methods and Calphad. Help speed the development and optimization of storage materials that can meet the 2010 DOE system target of 6 wt% and 45 g/L capacities.

- Characterize structures, compositions, hydrogen dynamics, and absorption-site interaction potentials for candidate storage materials.
- Provide Calphad calculations of phase relationships of potentially promising hydrides.

## *Detailed neutron studies in support of the Center's go/no-go analysis*

Month/Year	Milestone or Go/No-Go Decision
Apr-07 <b>(Complete)</b>	Milestone: Evaluate structural and bonding properties of new materials selected through discussions with the leadership of the Center. (Complete for Li-Si(Ge)-H, Ca-Si-H, and Na-Si-H systems)
Sep-07 <b>(Complete)</b>	Milestone: A thorough analysis as needed of the materials that are the most promising in terms of meeting the Phase 1 go/no-go decisions (Interest in, e.g., Na-Ge-H, $\text{Ca}(\text{BH}_4)_2$ and $\text{LiBH}_4$ in carbon aerogel)
Apr-08	Milestone: Evaluate structural and bonding properties of new materials selected through discussions with the leadership of the Center and coordinating council and establish a high-pressure hydrogenation system to complement work performed at SNL. Current systems of interest are Li-B-N-H, perovskite hydrides, $\text{Li}_2\text{B}_{12}\text{H}_{12}$ intermediates, scaffolded- $^7\text{Li}^{11}\text{BH}_4$ , $\text{LiKBH}_4$ , $\text{Ca}(^{11}\text{BH}_4)_2$ , and $\text{AlH}_3$ .
Sep-08	Milestone: A thorough analysis as needed of the materials that have favorably passed the Phase 1 go/no-go decisions and show the most promise of achieving the DOE 2010 targets (e.g., other nano-confined borohydrides).

## *Thermodynamic evaluations (Calphad)*

Month/Year	Milestone or Go/No-Go Decision
Jan-07 <b>(Complete)</b>	Milestone: Conduct evaluation of literature data for Li-Na-K alanate systems. For future development of the thermodynamic database, borohydride systems are given higher priority over alanate systems.
Sep-07 <b>(Complete)</b>	Milestone: Complete thermodynamic description for the Li-B and update database for Li-Mg-B-H.
Apr-08	Milestone: Develop description of the Ca-B-H system including the $\text{Ca}(\text{BH}_4)_2$ compound.
Sep-08	Milestone: Develop description of the Mg-B-H system including the $\text{Mg}(\text{BH}_4)_2$ compound.

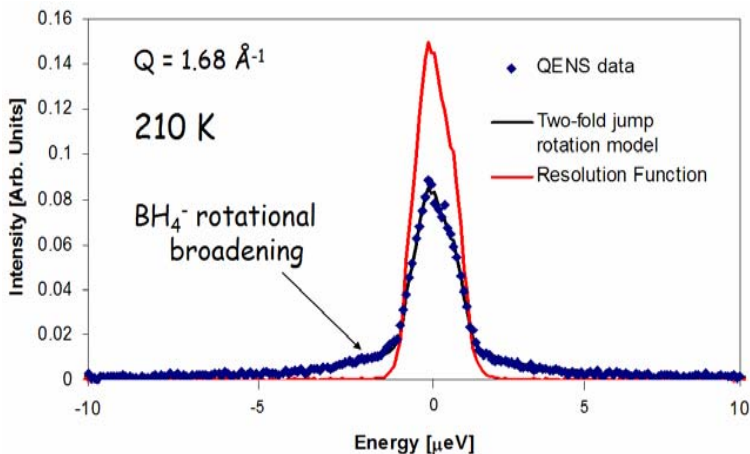
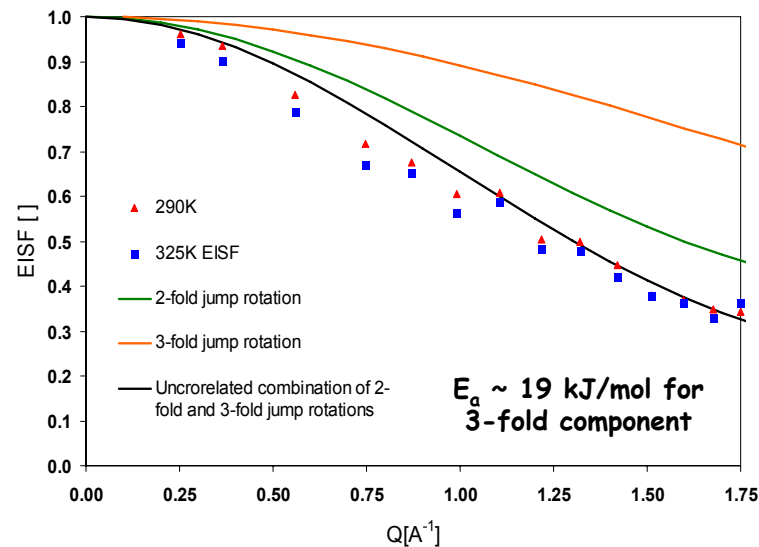
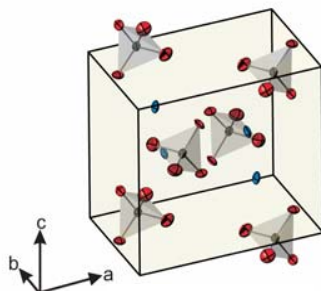
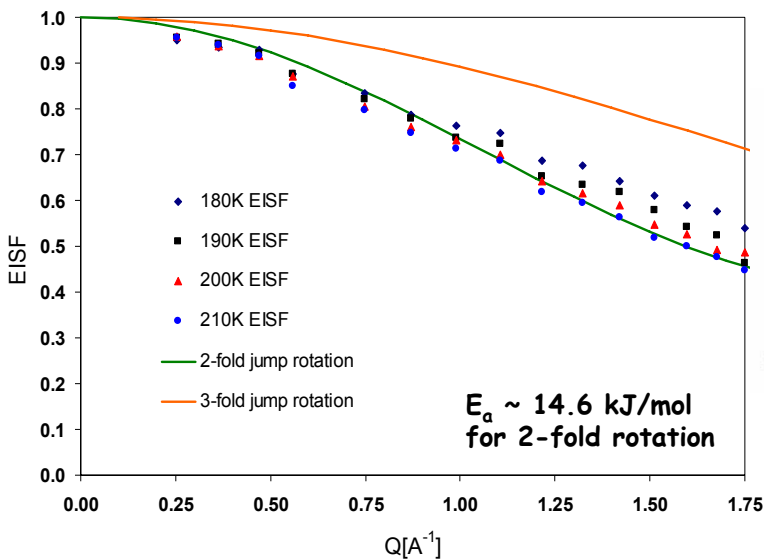
- **Neutron methods**

- determine elemental compositions of materials (prompt- $\gamma$  activation analysis and neutron reflectometry of H stoichiometries and profiles)
- determine location of H and crystal structures of materials (neutron diffraction superior to XRD for “seeing” light H and D)
- determine bonding of absorbed H (unlike IR and Raman, neutron vibrational spectroscopy “sees” all H vibrations for straightforward comparison with first-principles calculations)
- elucidate H diffusion mechanisms (faster dynamics timescale of neutron quasielastic scattering complements NMR; transport mechanisms gleaned from momentum transfer dependence)

- **Calphad methods**

- develop a thermodynamic database from the available literature and first-principles calculations
- incorporate database into an overall temperature-pressure-composition framework for multicomponent metal-hydrogen systems

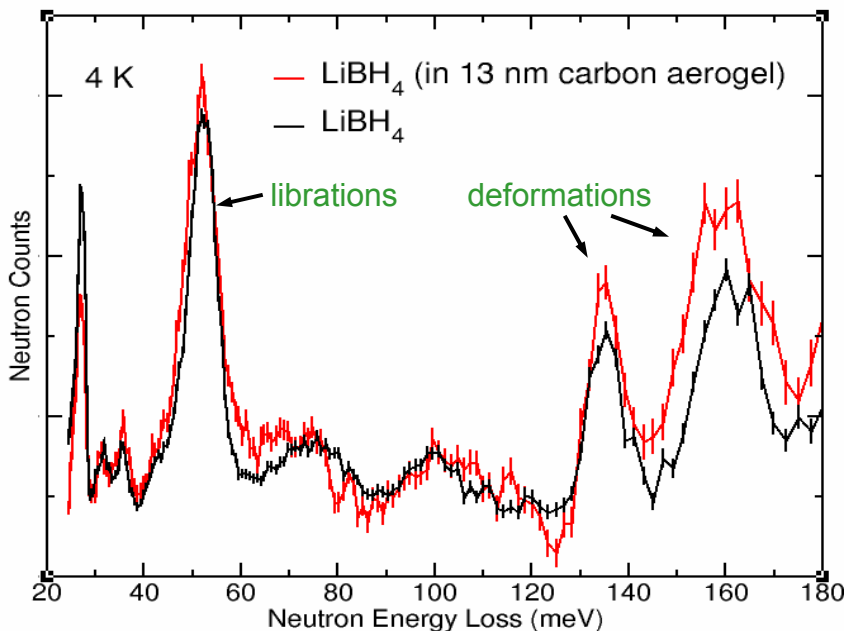
## Quasielastic Neutron Scattering of ${}^7\text{Li}{}^{11}\text{BH}_4$



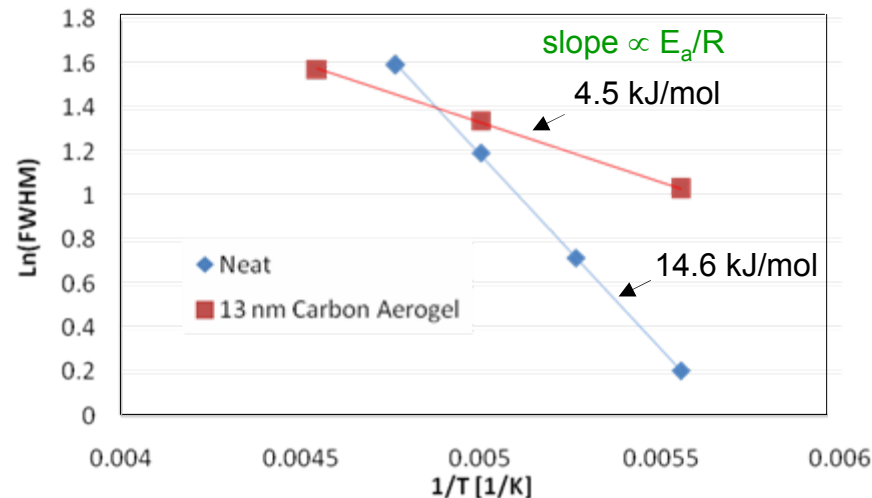
Quasielastic neutron scattering of  ${}^7\text{Li}{}^{11}\text{BH}_4$  indicates  $[\text{BH}_4]^-$  2-fold jump rotation near 200 K with an activation energy of  $\sim 14.6$  kJ/mol.

QENS data at 290 K and 325 K showed a departure from simple 2-fold rotation. An additional 3-fold rotation component with an activation energy of  $\sim 19$  kJ/mol is needed to fit the data.

## Effect of Nano-confinement on LiBH<sub>4</sub> Dynamics



Neutron vibrational spectroscopy (NVS) indicates minor broadening of LiBH<sub>4</sub> phonon modes due to nano-confinement in carbon aerogels with average pore sizes below 25 nm.



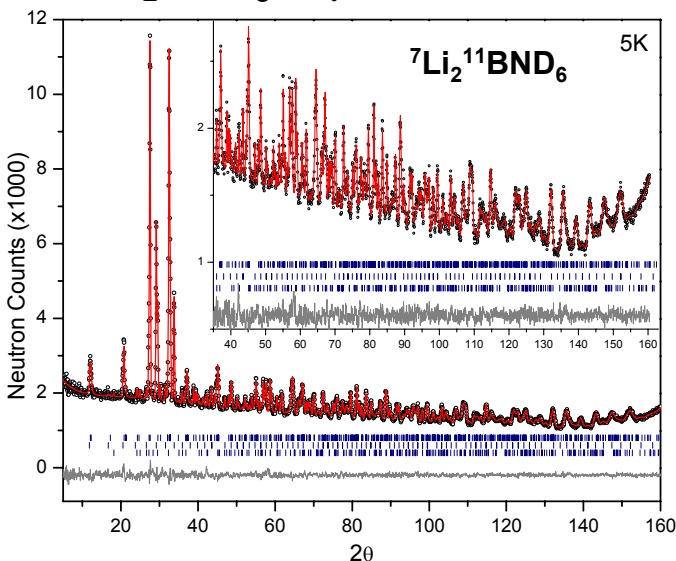
Quasielastic neutron scattering of neat and nano-confined <sup>7</sup>Li<sup>11</sup>BH<sub>4</sub> (in 13 and 4 nm carbon aerogels) indicates a significant change in [BH<sub>4</sub>]<sup>-</sup> rotational activation energies: 14.6 vs. 4.5 kJ/mol for neat vs. nano-confined.

Future studies will investigate the effect of both aerogel pore size and LiBH<sub>4</sub> fill fraction. These results will be used to develop a physical understanding of the enhanced rotational mobility and its relationship to improved cycling kinetics for these materials.

Motivation: A collaboration with HRL to investigate LiBH<sub>4</sub> dynamics perturbations in carbon aerogels

## Structures and Crystal Chemistry of $x\text{LiBH}_4 + (1-x)\text{LiNH}_2$ System

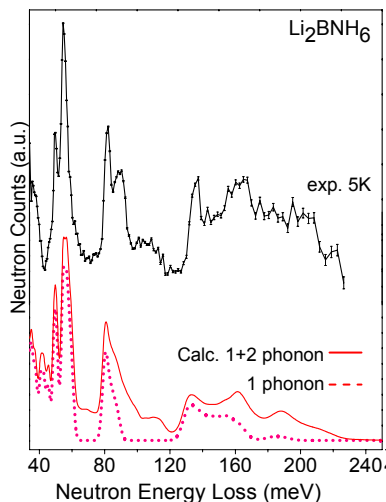
### $\text{Li}_2\text{BNH}_6$ crystal structure



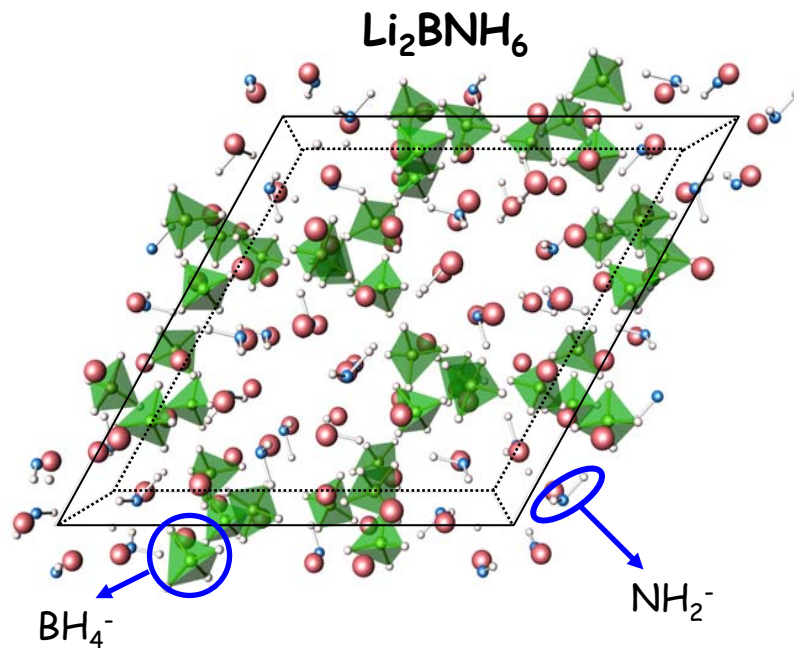
$^7\text{Li}_2\text{ }^{11}\text{BND}_6$  was used to determine the crystal structure of  $\text{Li}_2\text{BNH}_6$  by neutron powder diffraction.

The combination of neutrons and  $^7\text{Li}$  and  $^{11}\text{B}$  isotopes was essential for accurate structural results.

S. G. :  $R-3$  (No.148)  
 $a = 14.3944(3) \text{ \AA}$   
 $c = 9.0522(3) \text{ \AA}$



$\text{Li}_2\text{BNH}_6$  NV spectra and calculated phonon modes

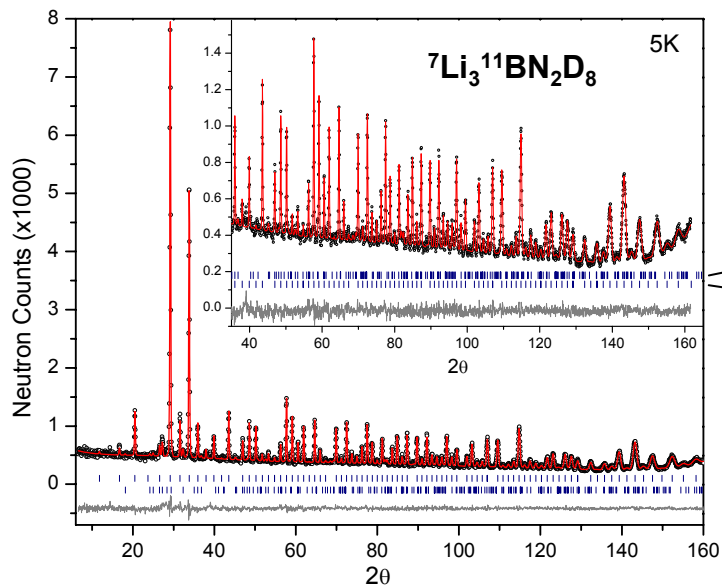


$\text{B-D1} \rightarrow 1.223 \text{ \AA}$	$\text{N-D5} \rightarrow 0.990 \text{ \AA}$
$\text{B-D2} \rightarrow 1.198 \text{ \AA}$	$\text{N-D6} \rightarrow 1.034 \text{ \AA}$
$\text{B-D3} \rightarrow 1.222 \text{ \AA}$	Mean N-D $\rightarrow 1.012 \text{ \AA}$
$\text{B-D4} \rightarrow 1.187 \text{ \AA}$	
Mean B-D $\rightarrow 1.208 \text{ \AA}$	

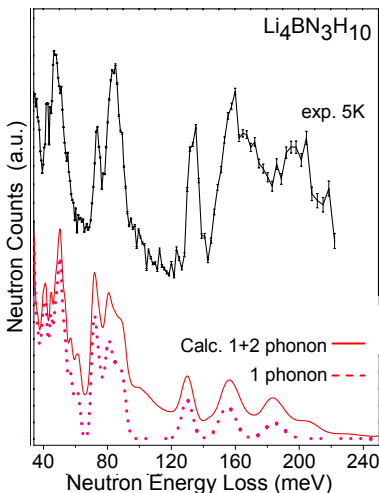
*\*Nearly ideal configuration found for both  $\text{BH}_4^-$  and  $\text{NH}_2^-$*

Motivation: Fundamental crystal chemistry information needed

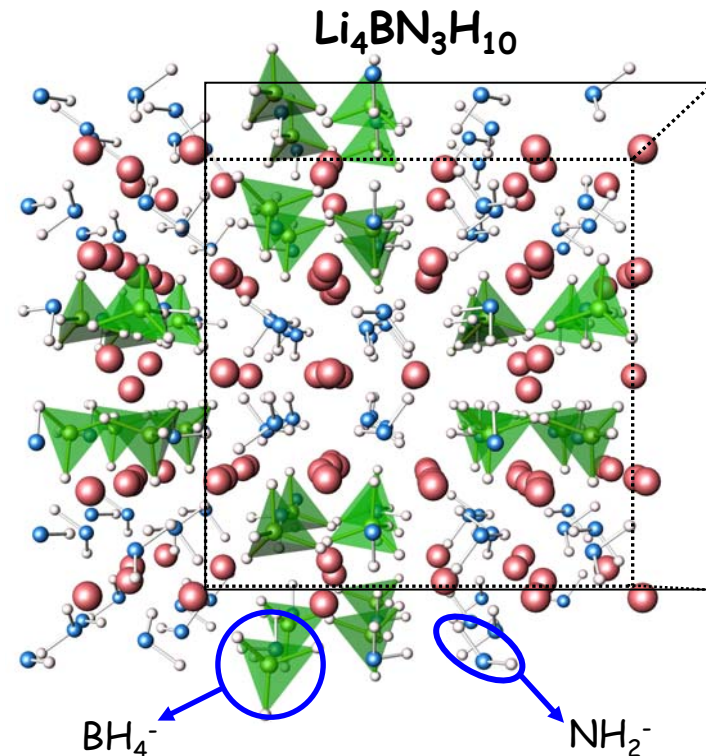
## Structures and Crystal Chemistry of $x\text{LiBH}_4 + (1-x)\text{LiNH}_2$ System



S. G. :  $I2_13$  (No. 199)  
 $a = 10.5803 (1) \text{ \AA}$



$\text{Li}_4\text{BN}_3\text{H}_{10}$  NV spectra and calculated phonon modes



B-D1 $\rightarrow 1.196 \text{ \AA}$	N-D5 $\rightarrow 0.996 \text{ \AA}$
B-D2 $\rightarrow 1.194 \text{ \AA}$ (3x)	N-D6 $\rightarrow 1.022 \text{ \AA}$
Mean B-D $\rightarrow 1.195 \text{ \AA}$	Mean N-D $\rightarrow 1.009 \text{ \AA}$

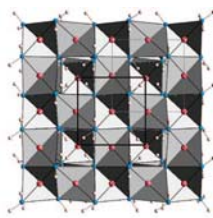
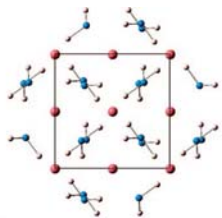
**\*Nearly ideal configuration found for both  $\text{BH}_4^-$  and  $\text{NH}_2^-$**

Neutron structural results indicate that  $\text{Li}_3\text{BN}_2\text{H}_8$  is not a single phase, but rather a combination of  $\text{Li}_4\text{BN}_3\text{H}_{10}$  and  $\text{LiBH}_4$ .

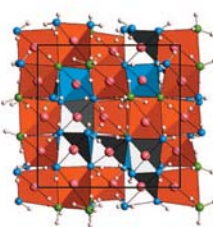
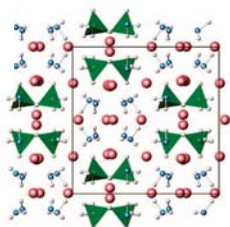
Again the combination of neutrons and  $^7\text{Li}$  and  $^{11}\text{B}$  isotopes was essential for accurate structural results.

## Li-B-N-H Quaternaries: A General View of $\text{Li}[\text{BH}_4]_x[\text{NH}_2]_{1-x}$

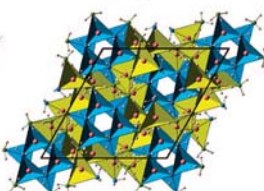
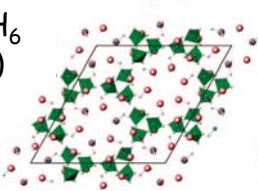
$\text{LiNH}_2$   
( $x=0$ )



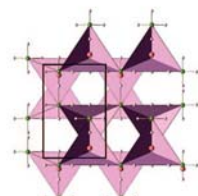
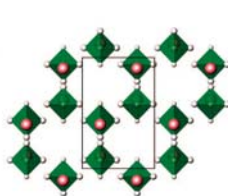
$\text{Li}_4\text{BN}_3\text{H}_{10}$   
( $x=0.25$ )



$\text{Li}_2\text{BNH}_6$   
( $x=0.5$ )

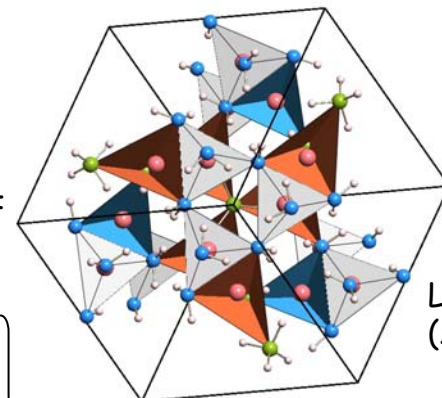


$\text{LiBH}_4$   
( $x=1$ )

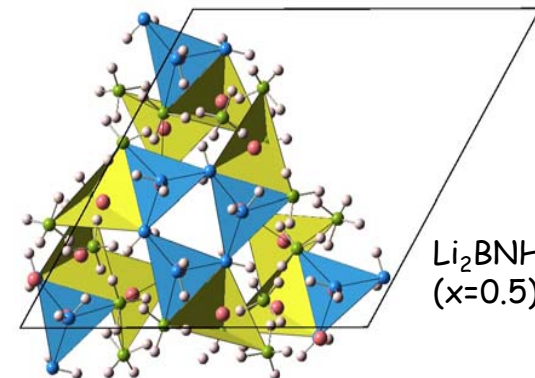


(at left) Structures are shown in both a ball-stick view containing  $\text{BH}_4^-$  units (in green) and  $\text{NH}_2^-$  units; and as polyhedral diagrams with  $\text{Li}^+$ -anion tetrahedra colored according to the different coordination environments of Li (see bottom row).

(at right) Comparison of  $\text{Li}_2\text{BNH}_6$  (half-shown for clarity) and  $\text{Li}_4\text{BN}_3\text{H}_{10}$  (viewed along  $[111]$ ) showing the structural progression of  $\text{Li}^+$ -anion tetrahedra upon replacement of  $\text{NH}_2^-$  with  $\text{BH}_4^-$ .



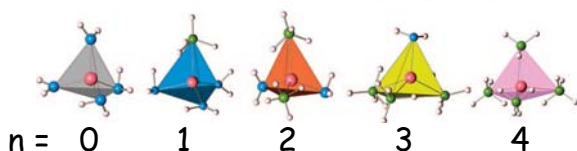
$\text{Li}_4\text{BN}_3\text{H}_{10}$   
( $x=0.25$ )



$\text{Li}_2\text{BNH}_6$   
( $x=0.5$ )

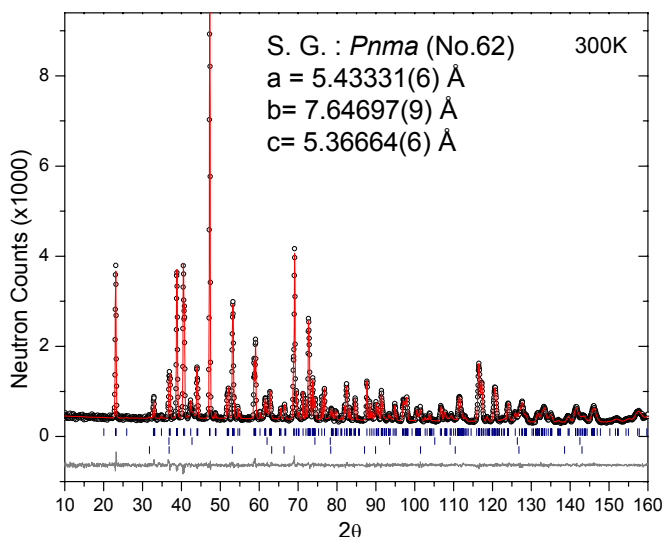
\* $\text{Li}^+[\text{NH}_2^-]_2[\text{BH}_4^-]_2$  tetrahedra are avoided in  $\text{Li}_2\text{BNH}_6$  due to steric instabilities.  $\text{BH}_4^-$ -rich quaternaries are also not observed for the same reason.

$\text{Li}^+[\text{NH}_2^-]_4$  tetrahedra are shown in gray,  $\text{Li}^+[\text{NH}_2^-]_3[\text{BH}_4^-]_1$  in blue,  $\text{Li}^+[\text{NH}_2^-]_2[\text{BH}_4^-]_2$  in orange,  $\text{Li}^+[\text{NH}_2^-]_1[\text{BH}_4^-]_3$  in yellow, and  $\text{Li}^+[\text{BH}_4^-]_4$  in pink.  $\text{Li}^+$  ions are shown as red spheres.

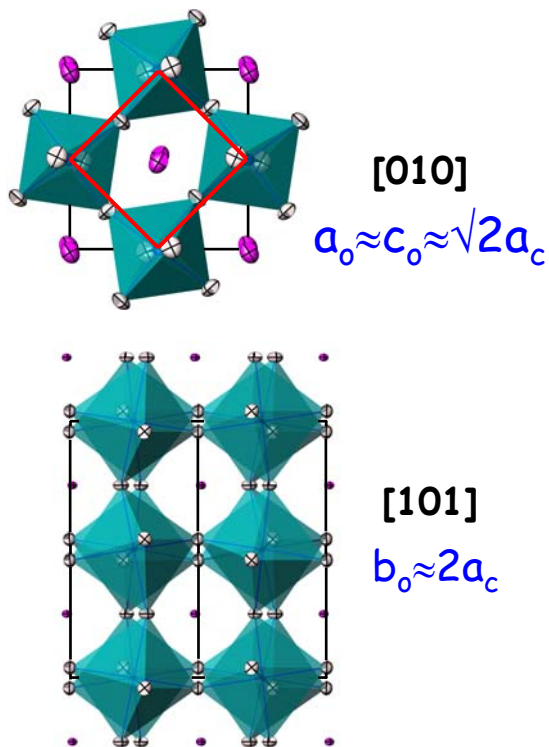


$\text{Li}^+[\text{BH}_4^-]_n[\text{NH}_2^-]_{4-n}$

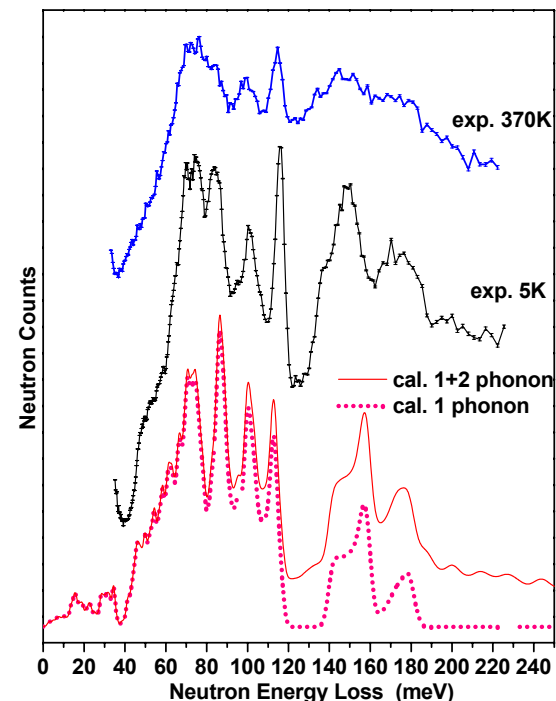
## Structure of NaMgH<sub>3</sub> from Neutron Powder Diffraction



Tolerance factor,  $t=0.93$ , leads to lattice distortion and octahedral tilting ( $\alpha b^* \alpha$ ) (*GdFeO<sub>3</sub>*-type orthorhombic perovskite structure).



Despite lattice distortion, nearly ideal MgH<sub>6</sub> octahedra are maintained.



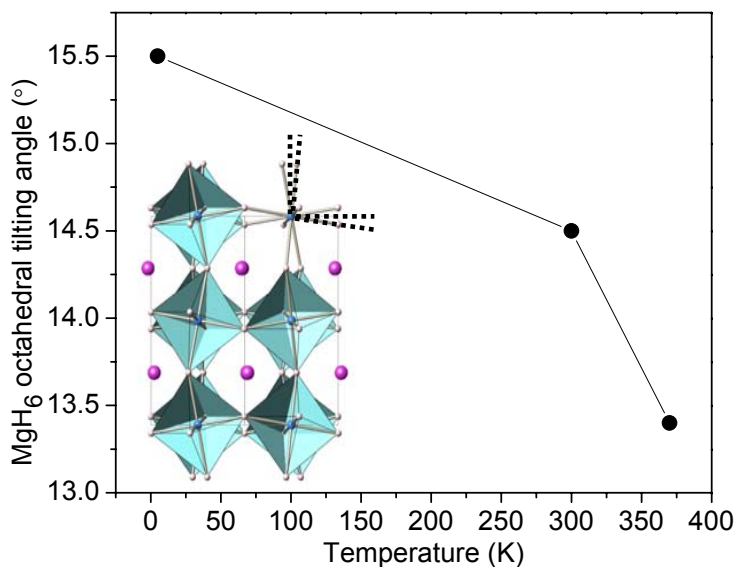
First-principles computations are consistent with observed NaMgH<sub>3</sub> phonon spectra.

Refined structure confirmed by DFT structural optimization and bond valence calculations.

Motivation: A collaboration with JPL to investigate origin of enhanced H mobility in perovskite with 6 wt.% H

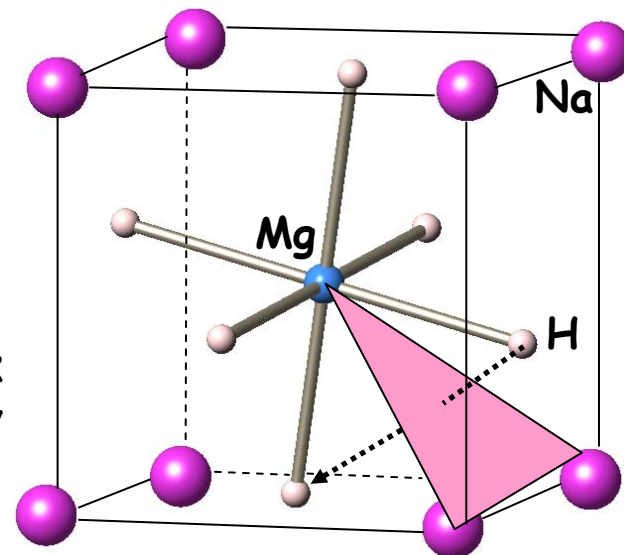
H. Wu, W. Zhou, T. J. Udovic, J. J. Rush, T. Yildirim, *Chem. Mater.* **20**, 2335 (2008).

## Structure Variation of NaMgH<sub>3</sub> vs. H Mobility with Temperature



No phase transition observed in 5-370 K range.

In perovskite oxides, more open bottleneck  $\approx$  higher ionic mobility



We observed a decrease in octahedral tilting angle with increasing T.

This is analogous to the behavior observed in perovskite oxygen ionic conductors.

Undistorted structure would have most open bottleneck.

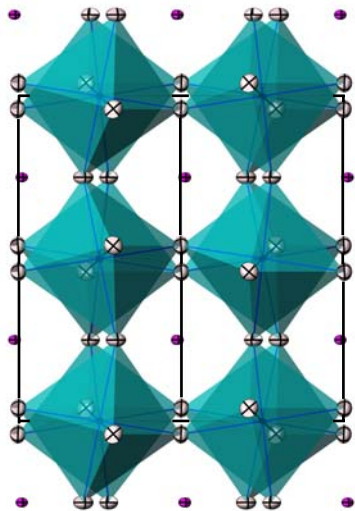
$\therefore$  H motion with lowest activation energy ( $E_a$ ) would result from smallest tilting angle.

The high H mobility observed by NMR with increasing T (H hopping rate  $\approx 3 \times 10^5 \text{ s}^{-1}$  at 573 K) is consistent with decreasing lattice distortion and octahedral tilting. Future focus should be on adjusting the structural characteristics so as to further increase H mobility.

## Implications for Hydrogen Storage



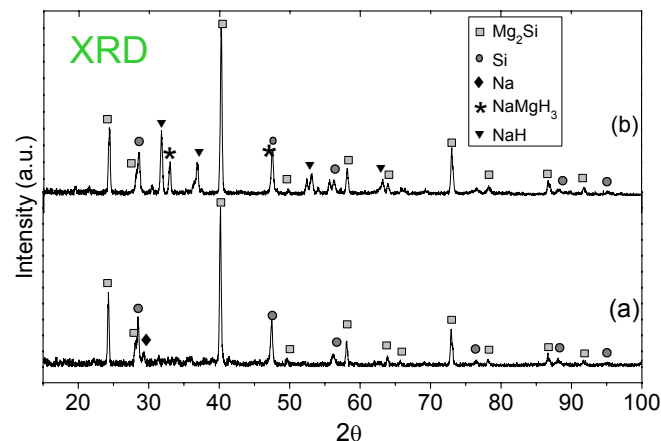
Reversible hydrogenation/dehydrogenation



MgH<sub>2</sub>/Si system is hard to hydride due to the kinetic limitations of MgH<sub>2</sub> (very slow intrinsic diffusion coefficient)

NaH/Si system reversibly absorbs H<sub>2</sub>

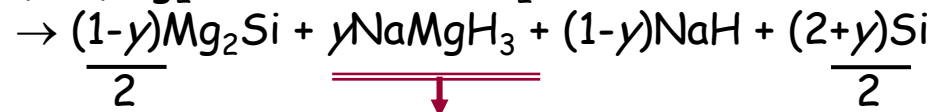
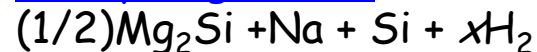
## What about the MgH<sub>2</sub>/NaH/Si system?



(a) Dehydrogenation: 623 K evac.

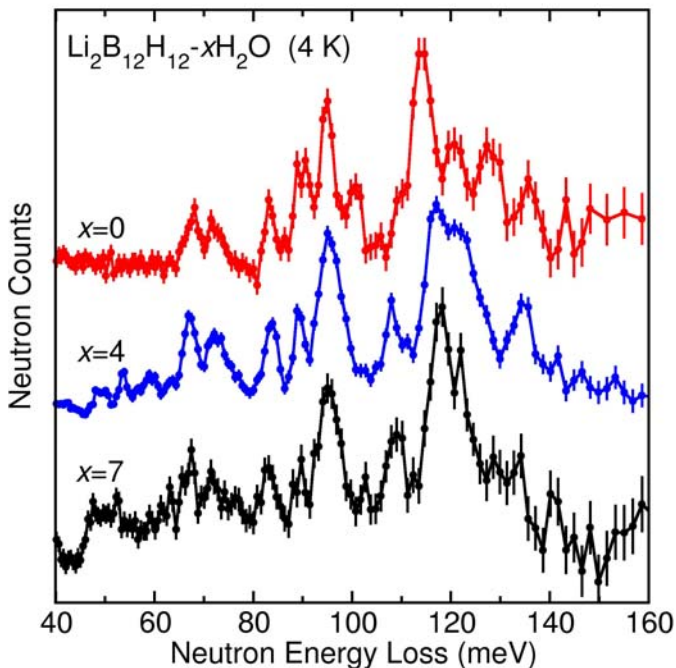


(b) Hydrogenation: 623 K, 50 bar H<sub>2</sub>

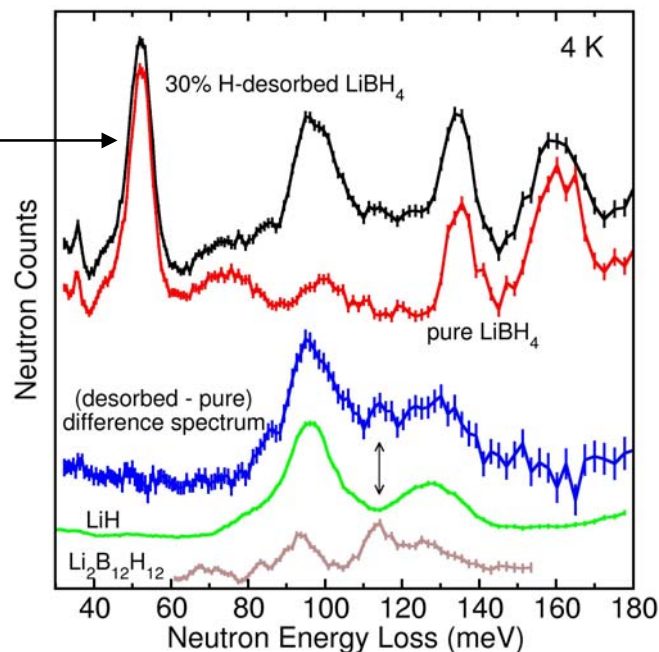


Mg<sub>2</sub>Si now "hydridable" through the formation of NaMgH<sub>3</sub> (perovskite-driven H mobility).

## Decomposition Products of $\text{LiBH}_4$ upon Partial $\text{H}_2$ Desorption



NV spectrum after pure  $\text{LiBH}_4$  was 30% dehydrogenated at 703 K into a fixed volume.

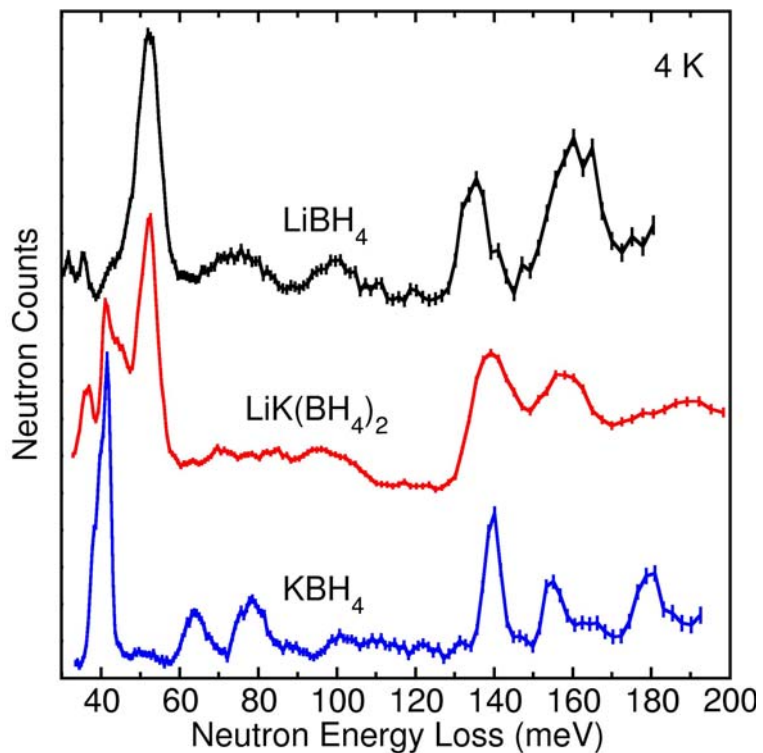


Pure  $\text{Li}_2\text{B}_{12}\text{H}_{12}$  was found to exist in two crystalline forms having four and seven waters of hydration.

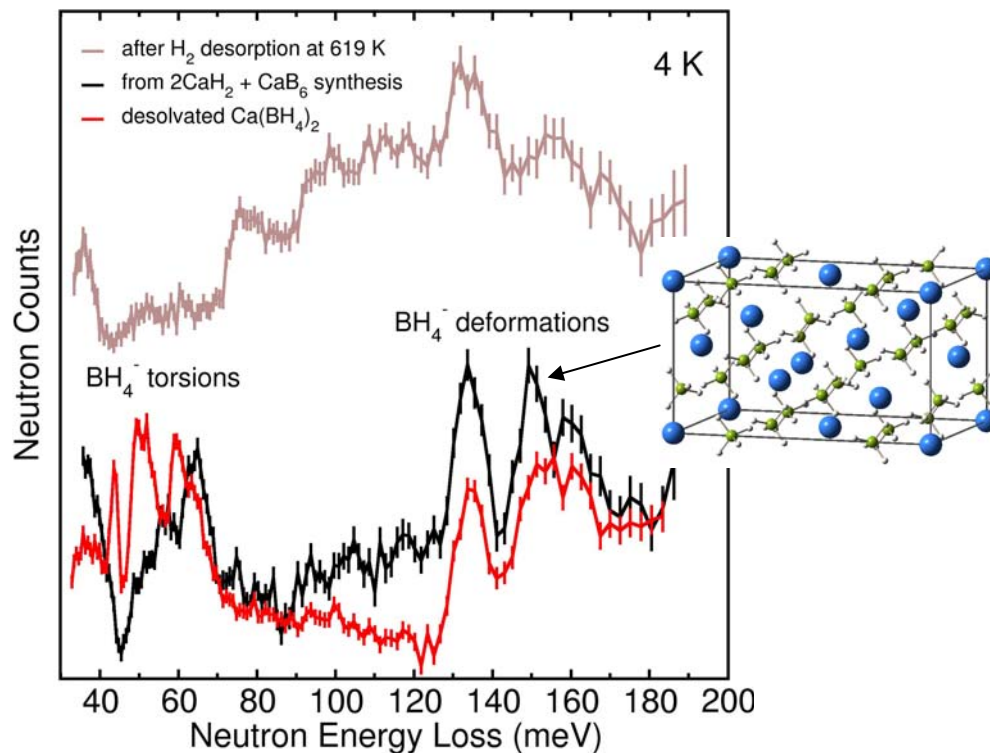
Anhydrous  $\text{Li}_2\text{B}_{12}\text{H}_{12}$ , formed by heating in air, was amorphous but yielded sharp  $(\text{B}_{12}\text{H}_{12})^{2-}$  phonon features.

Neutron vibrational spectroscopy results suggest the presence of an amorphous  $\text{Li}_2\text{B}_{12}\text{H}_{12}$  intermediate after partial dehydrogenation of  $\text{LiBH}_4$ .

## Neutron Characterization of MHCoe Samples: Novel Borohydrides

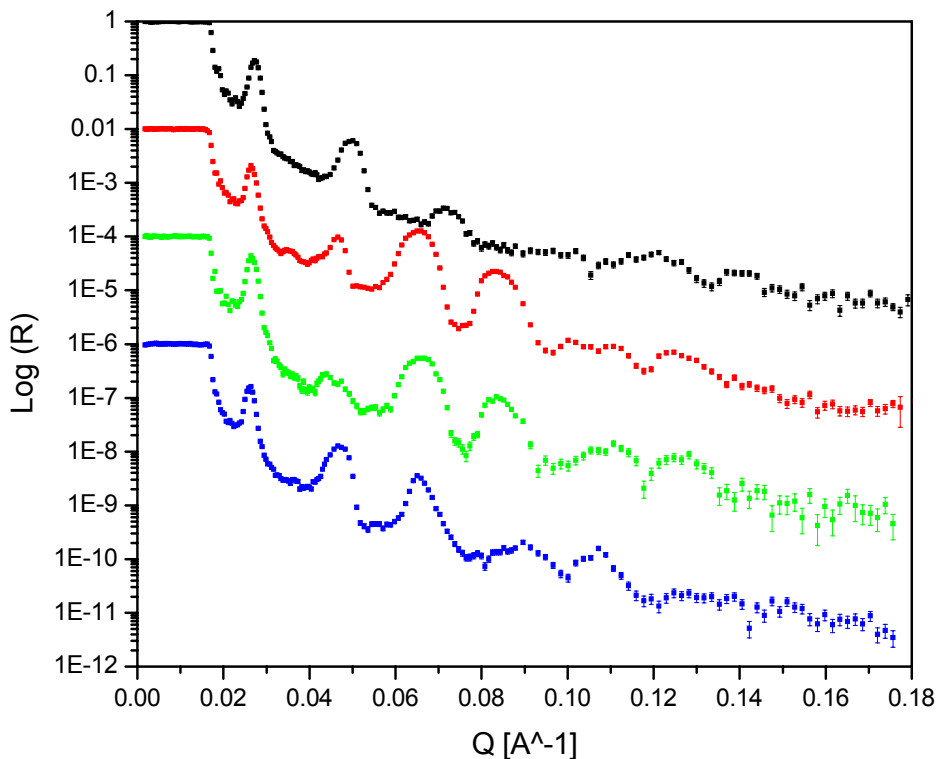


NV spectrum of  $\text{LiK}(\text{BH}_4)_2$  from SNL compared to those of  $\text{LiBH}_4$  and  $\text{KBH}_4$ . First-principles phonon calculations are underway to compare the optimized  $\text{LiK}(\text{BH}_4)_2$  structure with experiment.



NV spectra of different  $\text{Ca}(\text{BH}_4)_2$  samples from SNL. Torsional modes indicate that desolvated  $\text{Ca}(\text{BH}_4)_2$  possesses a different structure than observed above for sample synthesized from  $2\text{CaH}_2 + \text{CaB}_6$ .

## Hydrogen Concentration Profiling in Mg Films



Neutron reflectivity profiles of a thin-film multilayer comprised of 10 stacked Pd/Mg bilayers ( $50 \text{ \AA}/200 \text{ \AA}$ ) on a sapphire substrate.

Four measurements represent:

- (1) the as-received film
- (2) after 7.5 bar  $D_2$  exposure
- (3) after rt evacuation of deuterated film
- (4) after 353 K evacuation of deuterated film

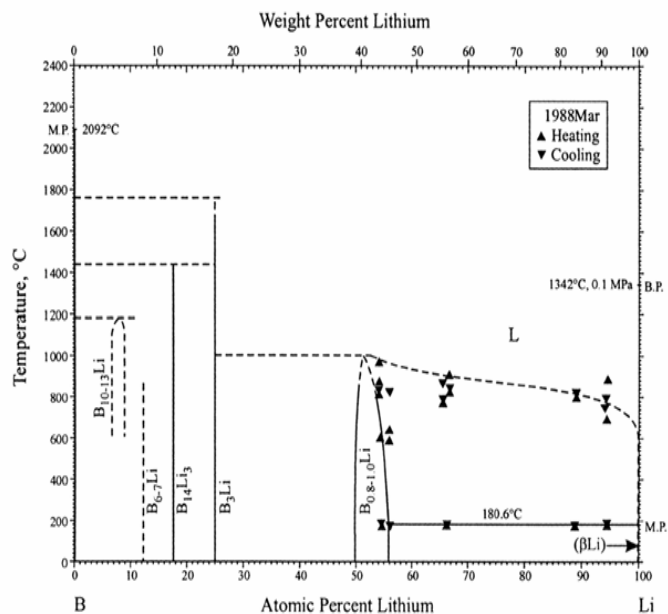
The sample did not go back to the as-received state after 353 K evacuation. Reasonable agreement was achieved using a model in which the amount of D in the Mg layers at room temperature increased linearly with layer number starting at the substrate, and a more even distribution of D in the Mg layers after heating to 353 K. This indicates that diffusion dominates over desorption at this temperature. Future measurements will be performed on single-layer films to study the D profiles with cycling.

Motivation: A collaboration with Stanford to help characterize hydrogen concentration profiles in thin films

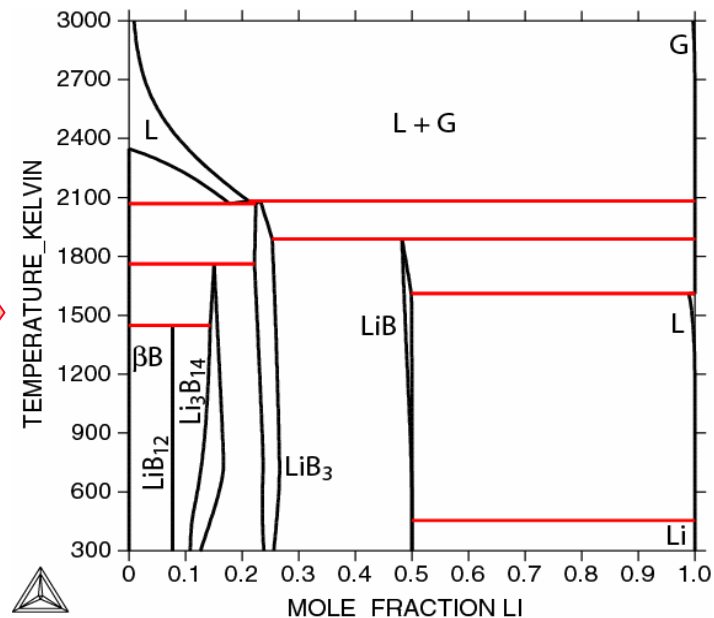
## Calphad Computations

- Development of Calphad database for H-Li-Mg-Ca-B-Si with thermodynamic descriptions of the constituent subsystems
  - Provisional descriptions of the constituent binary systems were replaced by refined model descriptions
- Challenge: lack of available experimental data
  - Incorporate data from first principles calculations from MHCoe partners

### Results: Binary System: Li-B



First principles  
& Calphad

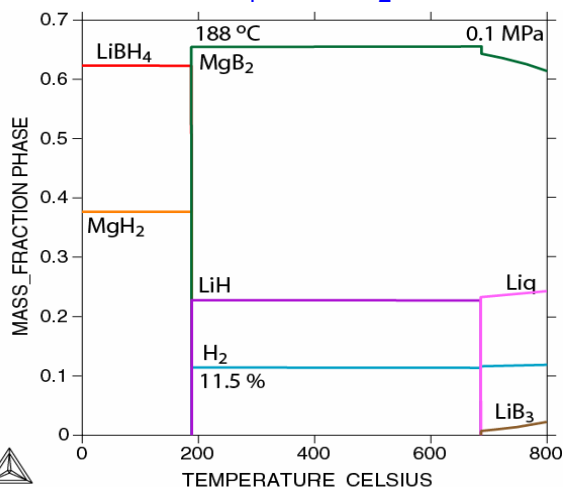


Motivation: A collaboration with the MHCoe theory group to develop thermodynamic databases of interest

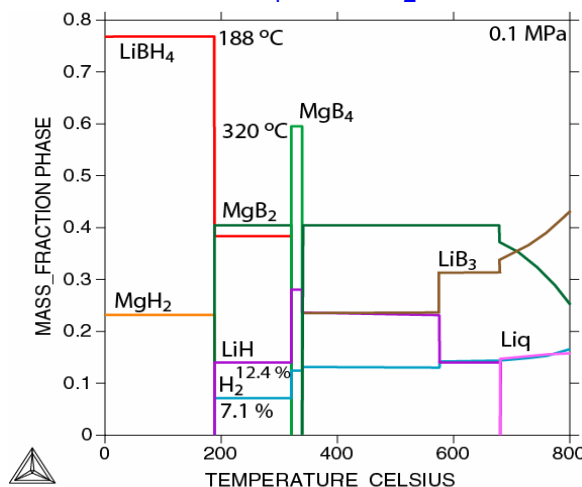
## Calphad Computations (continued)

### Results: Binary System: Li-Mg-B-H

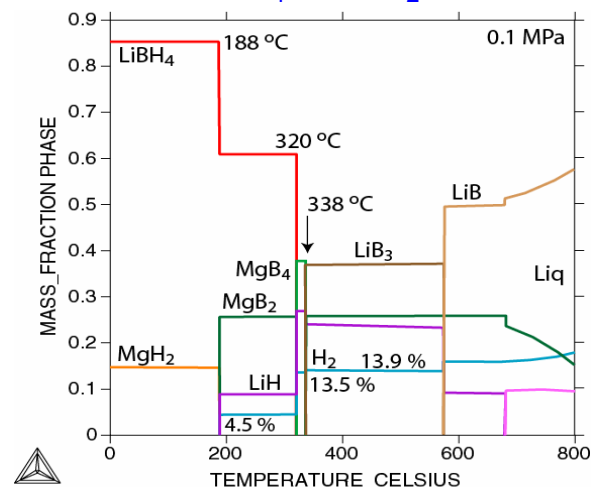
2 LiBH<sub>4</sub> + MgH<sub>2</sub>



4 LiBH<sub>4</sub> + MgH<sub>2</sub>



7 LiBH<sub>4</sub> + MgH<sub>2</sub>



The assessment of the Li-B system permitted consideration of the intermediate Li-B phases that were missing in the original calculations. >> Intermediate Li-B phases form during the dehydrogenation reactions of LiBH<sub>4</sub> with MgH<sub>2</sub>, but the most promising 2:1 ratio is not affected, as LiB forms only at high temperature.

## Remainder of FY 2008:

- Complete higher hydrogenation pressure capability (<1000 atm) and use to investigate new ternary and quaternary systems via neutron methods.
- Continue Mg thin-film characterizations using neutron reflectometry.
- Continue efforts to synthesize  $^{11}\text{B}$  labelled hydrogen-storage materials.
- Continue rotational dynamics investigations of borohydrides in aerogels.
- Develop Calphad description of the Ca-B-H and Mg-B-H systems including the  $\text{Ca}(\text{BH}_4)_2$  and  $\text{Mg}(\text{BH}_4)_2$  compounds.
- Identify systems with MHCoe partners for future neutron scattering studies and Calphad database development.

## FY 2009:

- Perform neutron scattering characterizations of new materials in conjunction with the needs of the other partners, including borohydrides and nanoscaffolded materials of interest.
- Continue to expand Calphad database (evaluate literature for data, identify data needs and systems with MHCoe partners for future database development).
- Initiate feasibility studies of unique neutron imaging of H distribution and transport in storage beds for candidate materials.

## Neutron methods and Calphad computations provided crucial, non-destructive characterization and predictive tools for the Metal-Hydride Center of Excellence.

- Quasielastic neutron scattering studies of  $\text{LiBH}_4$  nanoconfined in carbon aerogels indicated a higher  $\text{BH}_4^-$  rotational mobility than in the bulk with a significantly reduced rotational activation energy. Further studies will investigate the effect of both aerogel pore size and  $\text{LiBH}_4$  fill fraction on mobility and will be used to develop a fundamental understanding of the relationship between nano-confinement and improved cycling kinetics.
- $^7\text{Li}$ ,  $^{11}\text{B}$ , and D labelled samples were needed to accurately solve the crystal structures of  $\text{Li}_2\text{BNH}_6$  and  $\text{Li}_4\text{BN}_3\text{H}_{10}$ .  $\text{Li}_3\text{BN}_2\text{H}_8$  was found to be a mixture of  $\text{Li}_4\text{BN}_3\text{H}_{10}$  and  $\text{LiBH}_4$ . Nearly ideal configurations found for both  $\text{BH}_4^-$  and  $\text{NH}_2^-$  clarify the large discrepancies in prior reports on artificial anion distortions and inaccurate bond distances.  $\text{Li}[\text{BH}_4]_x[\text{NH}_2]_{1-x}$  compounds can be viewed as 3-D frameworks built by corner- and face-shared  $\text{Li}^+[\text{BH}_4^-]_n[\text{NH}_2^-]_{4-n}$  tetrahedra. Due to their promising H densities, further work will focus on their cycling properties under nano-confinement.
- Combined neutron and first-principles studies revealed the correct orthorhombic perovskite structure for  $\text{NaMgH}_3$ . Enhanced H mobility at elevated temperatures could be correlated with decreased lattice distortion and tilting of the  $\text{MgH}_6$  octahedra. Although the H desorption temperature is still too high for practical applications, improving H mobility in this class of hydrides would require (i) decreasing the lattice distortion and octahedral tilting via more favorable cation substitutions or other combinations of light elements and (ii) increasing the concentration of H vacancies via substitutional doping of Mg sites with monovalent cations.
- Neutron spectroscopy corroborated the formation of amorphous  $\text{Li}_2\text{B}_{12}\text{H}_{12}$  during the partial dehydrogenation of  $\text{LiBH}_4$ . Based on neutron and complementary NMR studies, the  $(\text{B}_{12}\text{H}_{12})^{2-}$  anion appears to be a common intermediate species during the dehydrogenation of other investigated borohydrides.

- Neutron reflectivity was shown to be sensitive to the hydrogen density profile through a thin Pd/Mg multilayer film on a sapphire substrate. Further studies will focus on determining the hydrogen density profiles associated with a single Mg layer during hydrogen cycling. This will give us a better handle on the fundamental mechanisms associated with H diffusion during hydriding.
- We have continued our primary task of performing various neutron characterization measurements in support of other MHCoe members.
- A Calphad database for H-Li-Mg-Ca-B-Si-N with thermodynamic descriptions of the constituent subsystems is being developed from literature data for the binary solution phases and intermediate compounds and data from first-principles calculations.
- The assessment of the description of the Li-B system permits more reliable predictions of reaction paths in systems containing these two elements.